

# Greenness-Driven Scheduling in Far Edge Kubernetes: A CODECO Evaluation

Kaikang Huang\*, Dalal Ali, Rute C. Sofia  
 fortiss GmbH – Research Institute of the Free State of Bavaria  
 Munich, Germany  
 {khuang, sofia}@fortiss.org, dalal@fortiss.org, dalal@fortiss.org  
 \*Corresponding author



**Abstract**—Energy consumption is an increasing concern in IoT-Edge-Cloud infrastructures, where containerized application orchestration must balance performance with sustainability. This paper investigates how the Kubernetes CODECO framework integrates cross-layer energy-awareness into scheduling decisions for containerized applications across the IoT-Edge-Cloud continuum. CODECO monitors energy at both the computational level, via Kepler, and a network (IP) level, and uses these metrics to define greenness heuristics that guide pod placement decisions through its ILP-based scheduler.

The approach is experimentally evaluated on a real-world far Edge testbed composed of ARM-based embedded devices, comparing CODECO against vanilla Kubernetes across multiple scenarios. The results show that CODECO consistently reduces the energy consumption of the cluster, with savings of up to 11.01 mJ in computational energy and 4.14 mJ in network transmission energy consumption at peak load, for a wide set of scenarios which combine different types of injected fault conditions, including CPU stress, asymmetric network delay, and bandwidth contention. A composite greenness score combining both energy dimensions provides a stable and consistent ranking of scheduling strategies across all conditions, demonstrating its suitability as a unified energy indicator for cluster-level orchestration decisions across the IoT-Edge-Cloud continuum.

**Index Terms**—Kubernetes, CODECO, Edge-Cloud continuum, resource management, energy-awareness

## 1 INTRODUCTION

The softwarization of network and computational resources has accelerated the decentralization of services across the Cloud-edge-IoT (CEI) continuum, pushing compute and data storage toward the far Edge, closer to a wide number of interconnected data sources. Large and complex applications, including AI models, can now be distributed across the CEI.

Existing orchestration mechanisms such as Kubernetes support deployment decisions based on Quality of Service (QoS) requirements such as CPU and memory. However, energy consumption has yet to be treated as a first-class requirement in the orchestration of applications across the CEI continuum. As the energy footprint of distributed computing infrastructures continues to grow, optimizing resource usage across both computational and network layers has become a pressing challenge.

To address this gap, the CODECO (Cognitive Decentralized Edge-Cloud Orchestration) framework based on

Kubernetes introduces an energy-aware orchestration approach that integrates cross-layer energy metrics directly into scheduling decisions [1], [2]. By jointly considering both computational and network transmission energy, CODECO enables a more intelligent workload placement that balances performance with energy efficiency, allowing applications to operate more sustainably while maintaining the responsiveness, reliability, and scalability required, for instance, in industrial environments, as is the case with Industrial IoT (IIoT) applications.

This work presents and evaluates CODECO’s cross-layer energy-aware scheduling approach considering far Edge environments. Greenness heuristics are introduced as scheduling cost functions that guide pod placement based on node-level energy profiles, and a composite greenness score is proposed as a unified indicator for cluster-level energy assessment. The approach is validated on a real far Edge testbed composed of ARM-based embedded devices, demonstrating measurable energy savings under a range of workload intensities and injected fault conditions.

This work makes three main contributions. First, it describes how CODECO monitors energy use across both computing hardware and network links, and feeds this information into Kubernetes to guide scheduling decisions. Second, it introduces and evaluates a set of “greenness” scores  $g(i)$  that combine network and compute energy data into a single measure of how energy-efficient a given application placement is. Third, it tests the approach on a real Edge testbed built from ARM-based embedded devices, showing that it uses less energy than standard Kubernetes scheduling under different workload sizes and failure conditions.

This paper is organized as follows. Section 2 describes related literature, highlighting the contributions of this work. Section 3 introduces the CODECO framework, focusing on the components that integrate energy-awareness into the scheduling pipeline. Section 4 describes the cross-layer observability approach that collects computational and network energy metrics, and introduces the greenness heuristics and scheduling cost functions. Section 5 presents the experimental setup, including the testbed, application, load generation, scenarios, and automation workflow. Section 6 presents the performance evaluation and analysis across proposed scenarios. Section 7 concludes the paper and pro-

poses directions for future research.

## 2 RELATED WORK

Resource scheduling in Kubernetes-based CEI infrastructures has been studied along two largely independent lines: energy-aware scheduling and network-aware scheduling. This section reviews representative work in each direction and identifies the gap that motivates the cross-layer approach presented in this paper.

### 2.1 Energy-Aware Scheduling

Energy-aware scheduling has emerged as a practical means of addressing the growing energy footprint of distributed edge-cloud infrastructures. Luo *et al.* [3] propose an energy-balancing task scheduling algorithm for container-based fog computing that dynamically assigns tasks according to the transmission energy states of edge nodes, balancing energy usage among heterogeneous nodes, and prolonging system lifetime. Their work establishes that incorporating energy metrics into scheduling decisions can significantly improve sustainability in resource-constrained environments, though it focuses on transmission energy alone and does not consider computational energy or Kubernetes-native orchestration.

More recent work has targeted power and carbon awareness directly within Kubernetes. Kepler [4] provides eBPF-based per-container power estimation by correlating hardware performance counters with energy measurements, exposing node and container-level power consumption through Prometheus. Although Kepler is a foundational monitoring tool — and is adopted in the present work — it does not itself influence scheduling decisions. Carbon-aware scheduling extensions [5] have explored using such measurements to trigger workload migration toward lower-carbon or lower-energy nodes, demonstrating that energy-aware rescheduling can improve cluster stability under high-load conditions and that composite energy models are better suited to heterogeneous hardware than single-metric approaches.

### 2.2 Network-Aware Scheduling

Incorporating network conditions into scheduling decisions has been recognized as an effective means of improving application performance in distributed environments. NetMARKS [6] enhances Kubernetes pod scheduling by collecting dynamic network metrics via Istio Service Mesh, achieving significant reductions in response time and inter-node bandwidth consumption in 5G and edge environments. However, NetMARKS optimizes network performance exclusively and does not consider energy efficiency or cross-layer scheduling.

Zeus [7] improves resource efficiency in large-scale Kubernetes clusters by enabling safe co-location of latency-sensitive and best-effort workloads, highlighting the importance of real-time resource utilization and interference awareness during scheduling. Like NetMARKS, Zeus does not incorporate energy-awareness into its scheduling logic.

NAS [8] proposes an eBPF-enabled network-aware Kubernetes scheduling framework that exploits fine-grained network metrics to guide placement decisions. While conceptually close to the network observability approach

adopted in this work, NAS focuses exclusively on network conditions and does not jointly consider energy consumption, limiting its ability to address energy-network trade-offs in heterogeneous CEI deployments.

### 2.3 Research Gap and Motivation

TABLE 1: Comparison of related scheduling approaches.

Approach	E-aware	N-aware	X-layer	K8s
Luo <i>et al.</i> [3]	Y	–	–	–
Kepler [4]	Y	–	–	Y
NetMARKS [6]	–	Y	–	Y
Zeus [7]	–	Y	–	Y
NAS [8]	–	Y	–	Y
CODECO [5]	Y	Y	Y	Y

Table 1 summarizes the key properties of the reviewed approaches. Although energy-aware and network-aware scheduling have each been extensively studied, orchestration frameworks that jointly consider both dimensions in a unified, cross-layer manner remain limited. Existing approaches typically optimise a single dimension, overlooking the strong interdependencies between energy consumption, network conditions, and workload placement in real-world CEI systems. In particular, no existing Kubernetes-native framework combines node-level computational energy estimation with flow-level network transmission energy in a single scheduling cost function, nor evaluates the trade-offs between these two dimensions under injected fault conditions on real embedded hardware.

This work addresses that gap by building on the CODECO framework [1] to introduce a cross-layer, composite approach that jointly considers computational and network transmission energy into scheduling cost functions and evaluates the resulting trade-offs experimentally on a real far Edge testbed under a range of workload intensities and fault conditions.

## 3 CODECO OVERVIEW

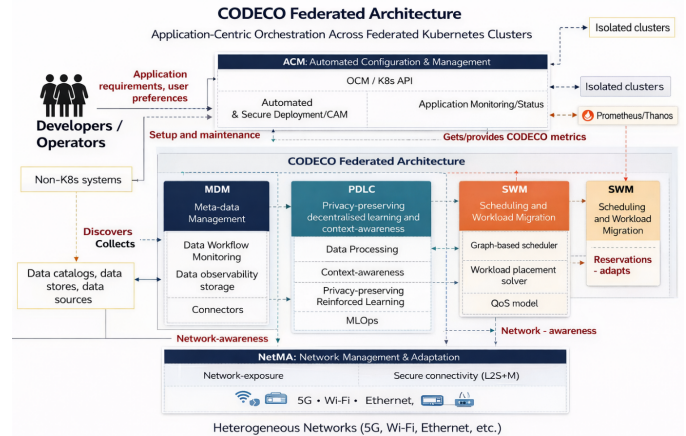


Fig. 1: The CODECO framework and its components.

CODECO<sup>1</sup> is a Kubernetes-based orchestration framework designed to extend Cloud-native application orchestration capabilities toward heterogeneous and dynamic CEI

1. <https://gitlab.eclipse.org/eclipse-research-labs/codeco-project>

environments. Its primary objective is to augment Kubernetes with cross-layer intelligence encompassing compute, network, and data dimensions, thereby enabling adaptive, context-aware, and efficient workload placement across the infrastructure continuum. The architectural overview of CODECO and its principal components is illustrated in Figure 1.<sup>2</sup>

At the heart of CODECO is the Advanced Configuration and Management (ACM) component, which automates both application setup and runtime adaptation. ACM is based on the RedHat Open Cluster Management (OCM)<sup>3</sup> solution. In addition to being the single CODECO interface to the user, it incorporates computational considerations into orchestration workflows, ensuring that deployments remain aligned with the operational characteristics of the underlying infrastructure. Central to ACM is the CODECO Application Model (CAM), a semantic description of an application’s micro-services and their *Quality of Service (QoS)* functional and non-functional requirements. CAM captures microservice dependencies, operational constraints, and target performance profiles such as resilience or greenness, which serve as high-level objectives guiding CODECO’s orchestration decisions across all components.

The Metadata Manager (MDM) brings data workflow observability to CODECO, maintaining consistent multi-layer snapshots of the system, capturing data dependencies, device status, and infrastructure changes that influence deployment and re-deployment decisions.

The Privacy-preserving Decentralized Learning and Context-awareness (PDLC) component enriches the orchestration pipeline with context-aware intelligence and AI-driven placement recommendations based on the performance profiles defined in CAM. It operates through two mechanisms:

- **Aggregated node and cluster scoring (PDLC-CA):** computes composite costs consistent with user-defined performance profiles.
- **System Stability Estimation:** applies Multi-agent Reinforced Learning (MARL) to detect potential instability in the infrastructure and issues scheduling recommendations intended to promote robust application deployment.

Workload placement is orchestrated by the Scheduling and Workload Migration (SWM) component, which provides a graph-oriented, ILP-based Kubernetes scheduler, that considers both application requirements (CAM) and the infrastructure state monitored by CODECO to compute a near-optimal placement solution. CODECO continuously monitors the infrastructure through ACM (compute), NetMA (network), and MDM (data), exporting all metrics to Prometheus<sup>4</sup> to allow seamless incorporation of new or user-defined metrics. For the purposes of this work, two perspectives are relevant:

- **Computational Perspective:** node-level energy consumption, resource availability, and device constraints, collected via Kepler and exported by ACM.

- **Networking Perspective:** underlay and overlay performance, link energy, flow energy, and inter-node connectivity, collected by NetMA.

## 4 CODECO OBSERVABILITY

The CODECO framework incorporates a cross-layer observability approach that integrates metrics from the application, data, and network domains to support context-aware orchestration across the CEI continuum. Measurements collected by ACM, MDM, and NetMA are exported to Prometheus for unified monitoring, analytics, and scheduling support. The observability layer serves three primary purposes: (i) providing real-time visibility into the state of the infrastructure, (ii) supporting metric-driven scheduling and workload migration through SWM, and (iii) enabling user-defined performance profiles such as energy-efficiency (*CODECO greenness*) or resilience.

By integrating Kubernetes-native metrics with CODECO-specific cross-layer measurements, the observability pipeline extends traditional cluster monitoring with additional insights from MDM and NetMA, as well as context-aware processing from PDLC. This allows SWM to correlate application behavior with infrastructure conditions in a unified manner, informing runtime decisions such as pod scheduling, migration, and scaling. Of the three observability categories described in this section, computational and network observability are directly relevant to the energy-aware scheduling approach evaluated in this paper.

This section describes the three main categories of observability supported in CODECO.

### 4.1 Application Observability

Application observability in CODECO builds on the native mechanisms provided by Kubernetes, which manages the lifecycle of containers, pods, and deployments. Through ACM, CODECO collects standard Kubernetes telemetry including pod status, readiness and liveness probes, container restart counts, resource requests and limits, and CPU/memory utilisation via the *Metrics Server* and *cAdvisor*. Additional signals include event logs, scheduling delays, QoS levels, autoscaling triggers, and application-level indicators such as request latency and error rates. Together, these metrics provide both fine-grained and aggregated visibility into application behavior and form the basis for application-level energy analysis by linking resource utilisation to computational energy consumption.

#### 4.1.1 Observability of Node Energy

Kubernetes does not natively expose power or energy metrics as part of its resource model. Node-level energy observability instead emerges from the integration of Kubernetes with operating system interfaces and external monitoring tools. Kubernetes contributes the execution context required for energy attribution, e.g., pod and container identifiers, *cgroup* hierarchies, and per-container resource usage from *cAdvisor* and the *Kubelet*, capturing CPU cycles, memory usage, I/O operations, and network activity, all of which correlate with dynamic energy consumption.

Actual energy measurements originate outside Kubernetes, through hardware and kernel interfaces such as Intel

2. A detailed overview of the CODECO federated orchestration capabilities is available in [9], [2].

3. <https://open-cluster-management.io/>

4. <https://prometheus.io/>

Running Average Power Limit (RAPL), Advanced Configuration and Power Interface (ACPI), or Baseboard Management Controller (BMC) mechanisms such as Intelligent Platform Management Interface (IPMI). Frameworks such as Kepler<sup>5</sup> bridge this gap by combining (i) hardware counters when available, (ii) kernel-level instrumentation via eBPF, and (iii) cgroup-scoped resource statistics from Kubernetes. Kepler correlates these sources to estimate node- and container-level energy consumption and exposes the results through Prometheus. CODECO relies on the same mechanisms to observe node energy, with Kubernetes providing the semantic structure for attribution and Kepler providing the measurements.

In the experimental testbed described in Section 5.1, all worker nodes are ARM-based embedded devices. This introduces important observability constraints. ARM-based devices such as Raspberry Pis typically lack the standard power telemetry interfaces available on x86 servers (ACPI, IPMI), and while ARM kernels support eBPF, the associated *BPF Type Format (BTF)* provides only minimal metadata without exposing hardware-level energy counters. Direct hardware energy measurements are therefore not available on these devices.

On x86 bare-metal environments with internal sensors, Kepler can directly access kernel power data and export accurate node and container power readings. Kepler also provides pre-trained power models derived from CPU and system-resource usage patterns [10], but these are architecture-specific and were trained on Intel<sup>®</sup> Xeon<sup>®</sup> processors. Applying them to ARM devices introduces inaccuracies due to different hardware characteristics.

The experiments presented in this paper adopt Kepler’s default x86-based power model as a practical approximation, sufficient to capture high-level energy trends for comparative evaluation while acknowledging the limitations on ARM hardware. More accurate estimation would require architecture-specific model training, as explored in [11]; where retraining is not feasible, empirical approaches such as those proposed by Pol et al. [12] provide an alternative for embedded platforms.

The node energy metric used in this work is collected via the following Kepler Prometheus query, which returns the cumulative dynamic energy consumed by a node over a five-minute interval, aligned with the sampling strategy used throughout the experiments:

```
increase(kepler_node_platform_joules_total{
  exported_instance="<node.name>",
  mode="dynamic"}[5m])
```

## 4.2 Data Observability

Data observability is managed through MDM, which monitors data location, lineage, freshness, access frequency, and transfer overhead between nodes and clusters, and tracks dependencies between datasets and microservices. These metrics support data-aware orchestration by ensuring workloads are placed near required data sources. Data observability is not the focus of the present work; the reader is referred to [2] for a detailed description.

5. <https://sustainable-computing.io/>

## 4.3 Network Observability

Network observability through NetMA provides visibility into connectivity and communication performance across heterogeneous networks including 5G, Wi-Fi, and Ethernet. NetMA exposes metrics such as latency, available bandwidth, jitter, packet loss, and energy, captured from both underlay and overlay viewpoints per node and per inter-cluster link. All metrics are exported to Prometheus, enabling the orchestration layer to avoid congested links, maintain QoS guarantees, and optimise energy-performance trade-offs. Within NetMA, the *Network State Management (NSM)* sub-component maintains an up-to-date view of the end-to-end network state across clusters.

### 4.3.1 MON Sub-system and Energy Monitoring

The *netma-nsm-mon (MON)* module is a sub-component of NetMA responsible for source-node network probing and aggregation of underlay metrics. MON builds on the open-source Kubernetes *k8s-netperf*<sup>6</sup> plugin, adapted and extended to support additional metrics, including energy-related ones. MON periodically monitor the parameters shown in Table 2 via a cron job.

All underlay metrics are collected at a Kubernetes worker-node level, as worker nodes are the only point in the system where application execution context and end-to-end packet visibility coexist. Network switches and routers observe only raw packets and cannot infer which pod, container, or service produced a flow. In contrast, worker nodes host the microservices and expose full visibility into their ingress and egress traffic. Metrics such as *uNodeBandWidth*, *uLatencyNanos*, *uPacketLoss*, and *uLinkEnergy* require correlating packets with the Kubernetes resources responsible for generating them, a linkage that intermediate network devices cannot provide.

Worker nodes also expose visibility across all active network interfaces, enabling monitoring of node degree, link failures, aggregated bandwidth, and link-level energy. These metrics are collected by MON and fed into PDLC-CA, which uses them together with computational energy from Kepler to compute the  $g(i)$  scheduling cost functions described in Section 4.

TABLE 2: Network metrics exported by MON.

Attribute	Description	Unit
nodeName	Node identifier	–
name	Link identifier	–
uLinkFailure	Link failure count	–
uPacketLoss	Packet loss rate	–
uNodeNetFailure	Link+endpoint failure sum	–
uNodeBandWidth	Total egress bandwidth	Mbps
uNodeDegree	Active link count	–
uLatencyNanos	Egress latency (EMA)	ns
uLinkEnergy	Energy per link (EMA)	W

### 4.3.2 Link Energy Estimation

MON adopts the linear energy model proposed by Feeney et al. [13], which estimates the energy consumed by a single

6. <https://github.com/leannetworking/k8s-netperf>

packet of size  $s$  (bytes) as in Equation (1):

$$e(s) = \beta_1 \cdot s + \beta_0, \quad (1)$$

where  $\beta_1$  is the incremental per-byte cost and  $\beta_0$  is the fixed cost associated with protocol control overhead (e.g. RTS/CTS/ACK exchange). Both coefficients depend on the communication mode and are determined experimentally.

The link energy  $l_e(i, j)$ , defined as the energy consumed by node  $i$  due to transmission across egress link  $j$  during a monitoring period  $T$ , is obtained by summing over all  $n$  packets observed on that link as provided by Equation (2):

$$l_e(i, j) = \sum_{p=1}^n e(s_p), \quad (2)$$

where  $s_p$  is the size of the  $p$ -th packet. This lightweight estimation method requires no particular hardware, making it appropriate for CODECO edge deployments.

#### 4.3.3 MON Example

Figure 2 illustrates a scenario in which a Kubernetes cluster consists of one master node and three worker nodes interconnected via Wi-Fi. Each worker hosts two daemon pods: i) a passive `k8s-netperf` pod containing the modified `netperf` binaries and `iPerf3`, and ii) an active monitoring pod responsible for executing network measurements and updating a `ConfigMap`. Periodic `ConfigMap` updates are performed (default: every five minutes), with the interval configurable by the developer.

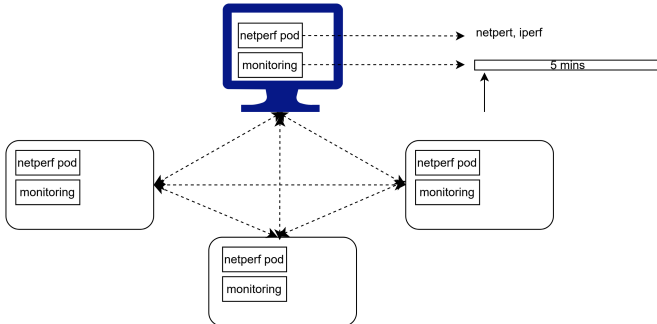


Fig. 2: MON example: cluster with four nodes.

#### 4.4 CODECO Greenness Metrics

Greenness in CODECO is a flexible concept that can be aligned with different sustainability objectives, including energy efficiency and CO<sub>2</sub> footprinting. In this work, greenness is defined as energy-awareness, encompassing energy consumption metrics collected at both the computational and network levels. The following energy-related metrics are considered:

- **Node Energy** ( $N_e(i)$ ): total energy consumed by node  $i$  across all its active processes, collected via Kepler using the eBPF-based query described in Section 4.
- **Link Energy** ( $l_e(i, j)$ ): energy consumed by node  $i$  due to the transmission of bits across egress link  $j$ , estimated by NetMA-MON using the linear power model of Equation 2.
- **Network Energy** ( $L_e(i)$ ): aggregate energy consumed across all egress links of node  $i$ :  $L_e(i) = \sum_j l_e(i, j)$ .

#### 4.5 Greenness Scheduling Functions

CODECO uses scheduling cost functions  $g(i)$  to rank nodes in terms of greenness. The cost value  $g(i)$  for each node is computed by PDLCA and passed to the SWM scheduler to guide pod placement decisions. Three formulations are exemplified with Equations (3,4,5):

$$g(i) = N_e(i) \quad (3)$$

$$g(i) = L_e(i) \quad (4)$$

$$g(i) = N_e(i) \cdot L_e(i) \quad (5)$$

Equation 3 captures a compute-centric view of greenness, ranking nodes solely by their total computational energy consumption. Equation 4 captures a network-centric view, ranking nodes by the aggregate transmission energy across all egress links. Equation 5 provides a composite view, jointly sensitive to both computational and network transmission energy, and to the number and cost of active links.

The choice of  $g(i)$  formulation defines the greenness performance profile applied during scheduling. The trade-offs between these three formulations are experimentally evaluated in Section 6.

## 5 EXPERIMENTAL SETUP

### 5.1 Experimental Environment

TABLE 3: Testbed equipment features.

Role	Device	Spec.	Node ID
Control plane	Laptop	16 Gi, 8 cores	master
Worker	RPI4	3.8 Gi, 4 cores	working0-2
Worker target	RPI4	3.8 Gi, 4 cores	working3-5

The experiments were conducted on a lightweight Kubernetes distribution, `k3s`<sup>7</sup>, deployed on a live testbed hosted at the fortiss IIoT Lab<sup>8</sup>. Figure 3 illustrates the experimental setup, including the positioning of CODECO within the testbed and their interaction with monitoring components. The setup consists of a single `k3s` cluster with one master node (a laptop) and six Raspberry Pi 4 corresponding to CODECO worker nodes as summarized in Table 3. A distinction is made between worker nodes that are used as target for application migration, and worker nodes where the application has been first deployed. The cluster is interconnected via a private IP network based on Wi-Fi (IEEE 802.11bg). The control node runs Ubuntu with kernel version 6.8.0-57-generic, while the worker nodes use a custom-built kernel (6.6.22-codeco-v8+) integrating eBPF hooks for energy monitoring through Kepler in Raspberry Pis.

Each node runs Kepler as a Prometheus exporter. Kepler leverages eBPF to collect CPU performance counters and Linux kernel tracepoints [4]. During the CODECO deployment (triggered by the ACM component), both Prometheus and Kepler are launched to monitor node-level compute energy metrics. The ACM component collects compute energy data from Kepler, while the NetMA component captures network energy consumption metrics. Both metrics are

7. <https://k3s.io/>

8. <https://www.fortiss.org/en/research/fortiss-labs/detail/iiot-lab>

continuously made available to PDLC and other CODECO components for cost evaluation (see section 3).

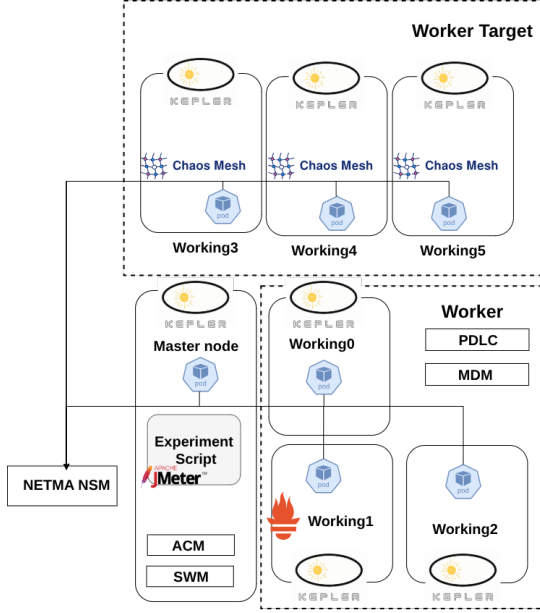


Fig. 3: CODECO testbed used in the experiments.

## 5.2 Application Setup and Load Generation

### 5.2.1 Application Bookinfo

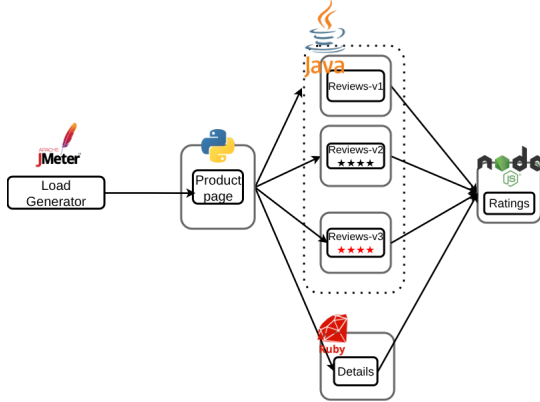


Fig. 4: BookInfo structure used in the experiments.

The application used in our experimentation is Bookinfo by Istio<sup>9</sup>, whose microservice topology is illustrated in Figure 4. Bookinfo comprises four micro-services: productpage, details, reviews, and ratings. In the baseline deployment, reviews is restricted to a single instance (v1), yielding four pods in total. To evaluate the impact of workload scaling on scheduling decisions, the number of reviews replicas is varied across experimental runs, as detailed in Section 5.3.

Application deployment is managed through the CODECO CAM YAML file (section 3), in which developers specify all the pods (micro-services) that compose an application and their interconnections<sup>10</sup>.

9. <https://istio.io/latest/docs/examples/bookinfo/>

10. The bookinfo CODECO yaml file used in experiments is available under [https://git.fortiss.org/iiot\\_external/experimentation/-/tree/main/CODECO-energy-awareness-benchmarking](https://git.fortiss.org/iiot_external/experimentation/-/tree/main/CODECO-energy-awareness-benchmarking)

### 5.2.2 Load Generation with JMeter

Apache JMeter<sup>11</sup> issues HTTP requests to the Bookinfo productpage microservice at a controlled rate expressed in *requests per second* (RPS), used here as a target load intensity. Three intensity levels are evaluated: 1 RPS (low), 15 RPS (medium), and 30 RPS (high).

RPS is configured via the *Throughput Shaping Timer*<sup>12</sup>, which paces request dispatch, and sustained by the *Concurrency Thread Group*<sup>13</sup>, which maintains the number of active threads needed to meet the target rate. Since thread demand depends on response time, the required thread count  $C$  is calculated as in Equation 6:

$$C = \frac{r \cdot t}{1000} \quad (6)$$

where  $r$  is the target RPS and  $t$  is the expected maximum response time in milliseconds (250 ms), ensuring threads remain active long enough to sustain stable pressure throughout each run.

## 5.3 Experimental Scenarios

Three progressive experimental scenarios are defined, each building upon the findings of the previous one: from workload characterisation under baseline conditions, through fault resilience evaluation, to a comparison of greenness scheduling strategies under combined stress.

### 5.3.1 Scenario I: Scalability and Load Characterisation

This scenario compares CODECO against vanilla Kubernetes across a range of workload intensities to identify the conditions under which each approach is most applicable. Two parameters are varied independently: the request rate (RPS) and the number of Bookinfo reviews micro-service replicas.

### 5.3.2 Scenario II: Edge Fault Resilience

With the workload fixed at RPS=30 and seven reviews replicas, this scenario aims at creating the dynamic and unpredictable conditions typical of real-world Edge deployments. Fault injection is performed using Chaos Mesh<sup>14</sup>, a cloud-native chaos engineering platform that integrates with Kubernetes to inject controlled faults at the pod, node, and network level. Four sub-scenarios of increasing severity are applied, as illustrated in Figure 5:

- **SII.1 - Baseline:** No fault injection; both schedulers operate under nominal conditions, establishing a reference for subsequent sub-scenarios.
- **SII.2 - CPU Stress:** StressChaos faults induce heterogeneous CPU contention across the three target worker nodes: 10% on worker3, 20% on worker4, and 50% on worker5, simulating resource-constrained edge nodes with varying degrees of degradation.
- **SII.3 - Network Delay:** NetworkChaos faults inject asymmetric latency across links: 75 ms on the worker3-worker4 link and 150 ms on both the worker3-worker5 and worker4-worker5 links, to

11. <https://jmeter.apache.org/>

12. <https://jmeter-plugins.org/wiki/ThroughputShapingTimer/>

13. <https://jmeter-plugins.org/wiki/ConcurrencyThreadGroup/>

14. <https://chaos-mesh.org/>

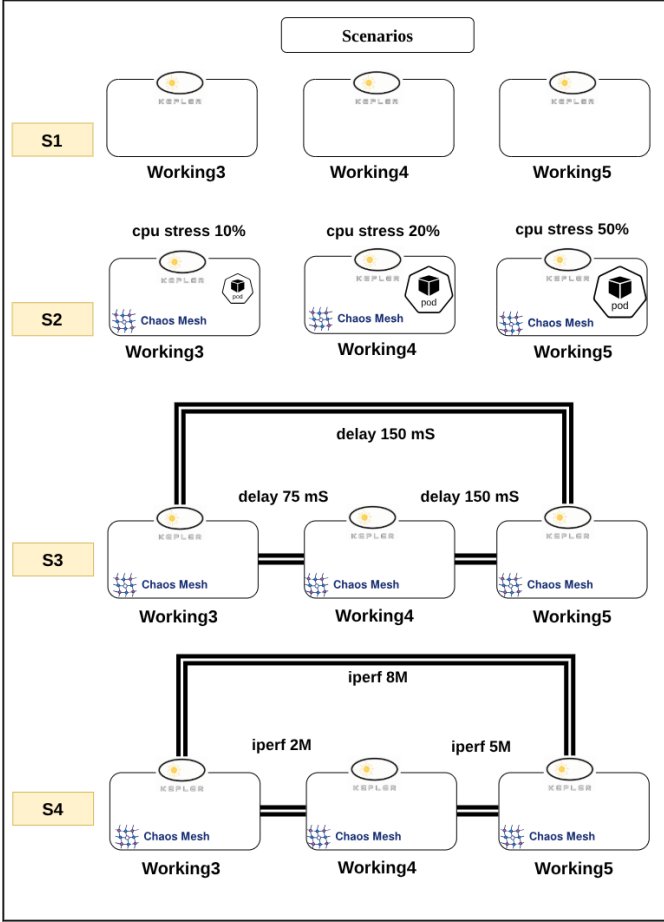


Fig. 5: Fault injection targets for Scenario II: (S1) baseline with no interference, (S2) StressChaos CPU stress on selected nodes, (S3) NetworkChaos latency injection on selected links, and (S4) NetworkChaos iPerf3 generating background traffic on selected links.

create conditions that could match geographically dispersed or unstable Edge connectivity.

- **SI1.4 - Controlled bandwidth contention:** `iperf3` background traffic saturates inter-node links with asymmetric loads: 2Mbps on worker3-worker4, 5Mbps worker4-worker5, and 8Mbps on worker3-worker5, simulating congestion conditions typical of a loaded far Edge network.

### 5.3.3 Scenario III: Greenness Scheduling Strategies Comparison

This scenario retains the same workload as Scenario II (RPS=30, seven reviews replicas) and fixes the interference conditions, namely, combined CPU and network stress applied via Chaos Mesh and `iperf`, while varying the  $g(i)$  scheduling function used by PDLC-CA to implement the Greenness performance profile. The three  $g(i)$  formulations provided in Equations (3,4,5) are evaluated:

- **Computational (comp):**  $g(i) = N_e(i)$ ; captures computational energy on the worker nodes without explicit consideration of inter-service network costs (Equation 3).
- **Network (net):**  $g(i) = L_e(i)$ ; captures the energy consumption due to IP packet transmission.

- **Composite (green):**  $g(i) = N_e(i) \cdot L_e(i)$ ; jointly captures both computational and network transmission energy consumption (Equation 5).

The outcome of each  $g(i)$  formulation is assessed across three cluster-level score metrics: computational energy, network energy, and the composite greenness score, which consolidates both dimensions into a single indicator.

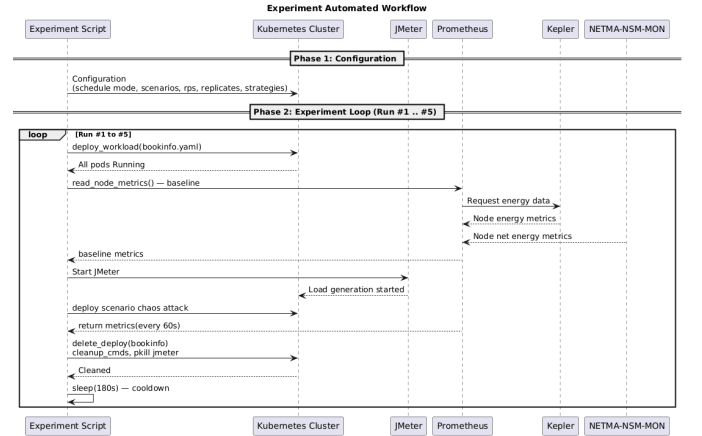


Fig. 6: Automated experimentation workflow.

## 5.4 Experimental Automation Workflow

To ensure reproducibility across configurations, all experiments were automated as detailed in the communication sequence diagram provided in Figure 6. All experiments were repeated at least five times at different times of the day to account for background activity variability. Results are reported as mean  $\pm 1$  standard deviation. Each run proceeds through the following steps:

- **Configuration.** Experimental parameters are parsed considering the scheduling approach (CODECO or default K8s), scenario (S1-S5), number of replicas, RPS intensity, and energy-awareness strategy (green, comp, or net). Then the corresponding strategy resource is deployed to the cluster.
- **Pre-clean.** All existing application workloads and ACM resources are removed to ensure a clean cluster state. `DaemonSet` pods such as Kepler and k3s system services remain active throughout.
- **Workload deployment.** Either the CODECO-managed or default Kubernetes Bookinfo deployment is applied, and the script waits until all pods reach Running state before proceeding.
- **Baseline energy collection.** A pre-load snapshot of node-level energy metrics is collected by Kepler.
- **Load generation and monitoring.** Apache JMeter generates foreground HTTP traffic at the configured RPS targeting the Bookinfo `productpage` microservice. Concurrently, a LiveMonitor records per-node energy and scheduling metrics every 60s into a timestamped CSV file. For scenarios with background interference (S2-S5), CPU stress and/or `iperf` network load is additionally injected via Chaos Mesh.

- **Post-load collection.** After a 600s monitoring window, post-load energy metrics are collected from Prometheus/Kepler.
- **Cleanup and cooldown.** All workloads and background stress processes are terminated, and the cluster is allowed a 180s cooldown before the next run begins.

To quantify the impact of the CODECO energy-aware scheduling strategy relative to the plain Kubernetes scheduler, the energy increase index  $ei$  is defined in Equation 7 as the relative increase in cluster energy consumption from the pre-deployment baseline  $e_{s1}$  to the post-deployment steady state  $e_{s2}$ :

$$ei = \frac{e_{s2} - e_{s1}}{e_{s1}} \cdot 100 \quad (7)$$

## 6 PERFORMANCE EVALUATION AND ANALYSIS

### 6.1 Scenario I: Scalability and Load Characterisation

**Scalability: impact of replica count.** As shown in Figure 7, the energy behavior of the two frameworks diverges increasingly with replica count. Table 4 provides a summary of the mean energy consumption gains across all use-cases.

With a single replica, CODECO and vanilla Kubernetes produce comparable computational and network energy across all RPS intensities. This is expected, given that a single replica offers no co-location opportunity and both schedulers make equivalent placement decisions in what concerns energy consumption. However, when the replica count increases, K8s exhibits higher and more variable computational energy, particularly for the scenarios with lower RPS intensity, while network transmission energy diverges progressively as RPS increases. For instance, for 7 replicas, K8s scales steeply in computational energy with both replica count and RPS, whereas CODECO remains comparatively stable. The same pattern of behavior occurs for the net strategy.

The key difference is that CODECO scheduler relies on an ILP-based solver that provides a solution for an application and its micro-services. Hence, replicas are consolidated onto nodes that already host communicating peers. Fewer active nodes means lower aggregate idle and dynamic power. In contrast, K8s targets load-balancing and therefore schedules each pod independently, balancing CPU/memory requests across nodes, which tends to spread replicas and keep more nodes partially loaded and may result in a less energy-efficient operating point. Hence, for larger numbers of replicas, this becomes a disadvantage. For instance, for the case of seven replicas, they are possibly distributed across the target nodes to assure better load distribution, whereas CODECO consolidates them on a few nodes.

In regards to the network energy target (net), co-located replicas communicate via loopback interfaces rather than the Wi-Fi interface, eliminating the per-packet transmission energy entirely for intra-node flows. On the Wi-Fi testbed (IEEE 802.11bg), inter-node communication carries a non-negligible energy cost per packet. As K8s adds replicas across nodes, the volume of Wi-Fi traffic grows proportionally. CODECO’s network-aware cost function explicitly penalizes link energy, so the scheduler actively avoids placements that generate inter-node flows.

**Load Characterisation: impact of RPS.** RPS is the primary driver of network energy differences between the two frameworks, and this can be better observed in Table 4. Across all replica counts, the gap between CODECO and K8s widens as the request intensity increases, and this effect is most visible for a larger number of replicas (rf. to Figure 7(c)). An increase in RPS increases the packet rates of active IP flows (more packets per second, higher dynamic and static energy costs), hence directly increasing link energy for the linear power model provided in Equation 2.

Computational energy also rises with an increase in the RPS intensity. However, the per-request CPU work (HTML rendering, database lookup in Bookinfo) is small and does not scale with request rate in a way that materially increases node power draw. The combination of high RPS and high replica count is therefore a worst-case for K8s (and a best case for CODECO), as it simultaneously maximises both the number of inter-node flows and their packet rate .

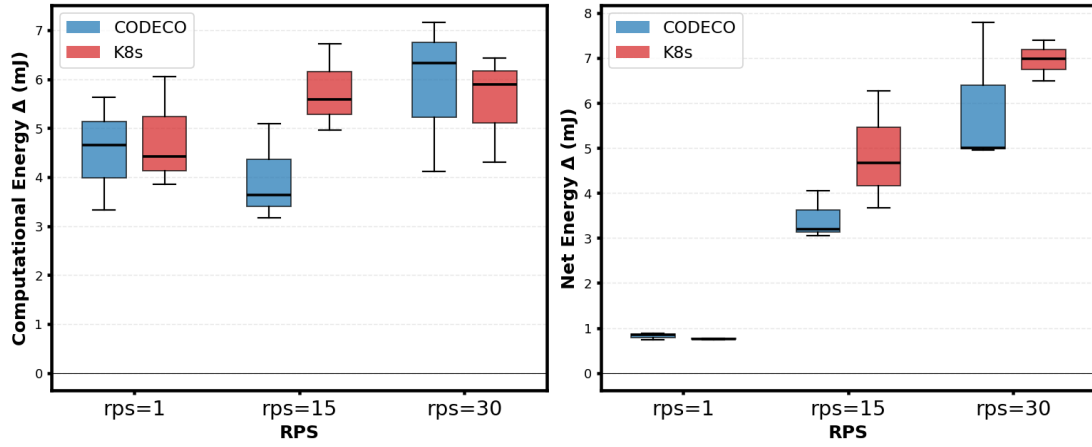
### 6.2 Scenario II: Edge Fault Resilience

Figure 8 presents the time-series evolution of cluster energy and network transmission energy across sub-scenarios SII.1–SII.4 at the operating point with rep equal to 7 and RPS equal to 30. Each chart reports mean values across repeated runs with one standard deviation bands. Experiments were run for 600 s.

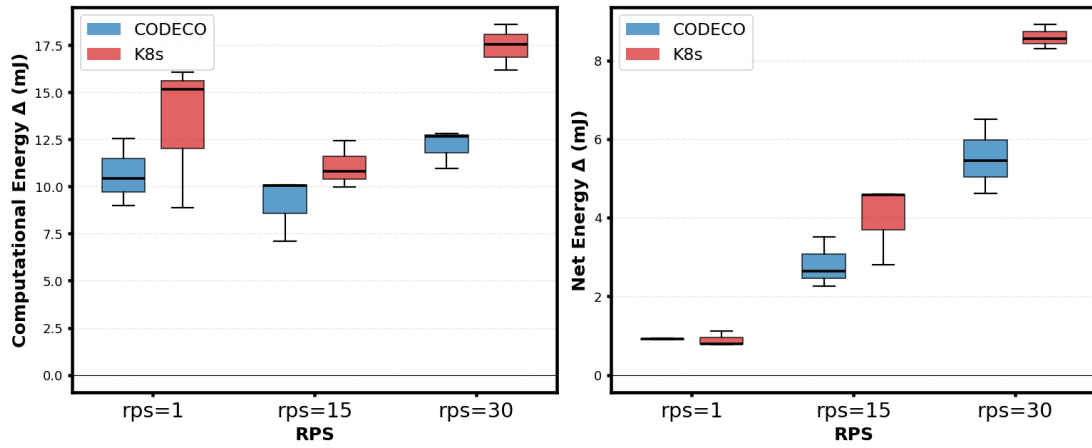
**SII.1 Baseline.** Under nominal conditions, CODECO maintains a stable compute cluster energy of approximately 21 mJ throughout the 600s window, compared with approximately 29 mJ for K8s. This indicates that CODECO consistently requires less compute energy while exhibiting a similarly stable temporal behavior. Network energy is also stable: CODECO remains at approximately 5.5 mJ, whereas K8s stays around approximately 10 mJ. This baseline establishes the reference separation attributable solely to placement strategy under undisturbed conditions.

**SII.2 CPU Stress Impact.** Under `StressChaos` faults, CODECO exhibits a pronounced dip-and-recovery pattern in compute cluster energy. This behavior appears to be related to the following operation. Upon detecting CPU stress, workloads are migrated to less-loaded nodes, causing Kepler telemetry to temporarily underestimate cluster consumption as pods transition. This produces the sharp drop to approximately 22 mJ near 100 s. Energy then rises toward the post-migration steady state and converges close to K8s, with both systems operating at approximately 34 mJ. The wide error bands that CODECO exhibits during the early migration window reflect run-to-run variability in migration timing. Hence, the initial compute-energy advantage is significantly reduced under CPU stress once migration completes, as both K8s and CODECO possibly operate on similarly loaded nodes. For network energy, CODECO remains consistently lower than K8s, suggesting that co-location is preserved across the migration event and that the transmission-efficiency gap is maintained.

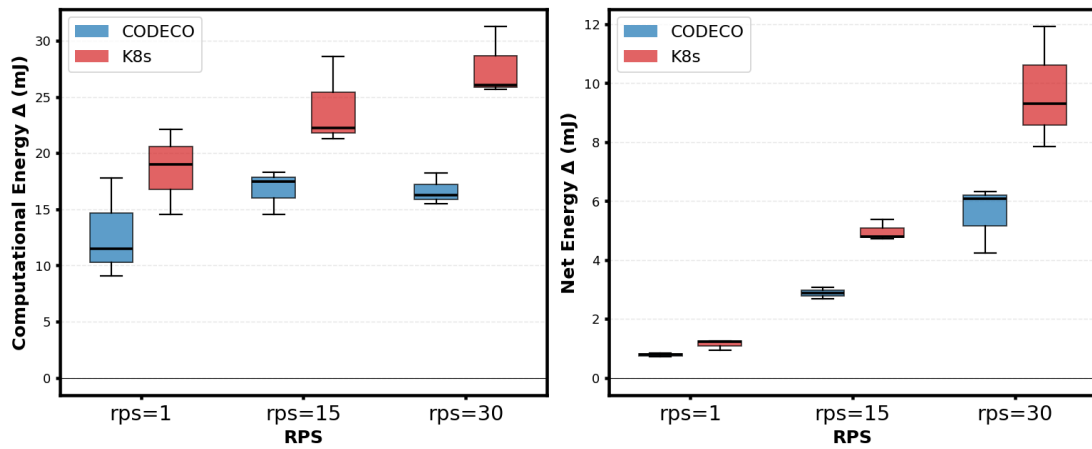
**SII.3 Network Delay Impact.** Under `NetworkChaos` latency injection, both time-series remain flat. With CODECO, the resulting cluster compute energy remains at approximately 23 mJ, compared with approximately 28 mJ for K8s. CODECO also maintains lower cluster network energy, at approximately 6.5 mJ against approximately 9 mJ for K8s.



(a) rep = 1



(b) rep = 4



(c) rep = 7

Fig. 7: Computational and network energy boxplots across  $RPS = \{1, 15, 30\}$  for replica counts of 1 (a), 4 (b), and 7 (c).

TABLE 4: Average energy consumption  $\pm$  standard deviation (mJ) and CODECO saving ( $\Delta = \text{K8s} - \text{CODECO}$ ) across replica counts and RPS intensity.

Replicas	RPS	Compute Energy (mJ)			Network Energy (mJ)		
		CODECO	K8s	Saving	CODECO	K8s	Saving
1	1	4.54 $\pm$ 1.16	4.78 $\pm$ 1.14	0.24	0.82 $\pm$ 0.08	0.76 $\pm$ 0.02	-0.06
	15	3.97 $\pm$ 1.00	5.76 $\pm$ 0.89	1.79	3.44 $\pm$ 0.54	4.87 $\pm$ 1.31	1.43
	30	5.87 $\pm$ 1.57	5.55 $\pm$ 1.10	-0.32	5.92 $\pm$ 1.62	6.96 $\pm$ 0.45	1.04
4	1	10.67 $\pm$ 1.80	13.37 $\pm$ 3.91	2.70	0.92 $\pm$ 0.02	0.89 $\pm$ 0.19	-0.03
	15	9.08 $\pm$ 1.73	11.08 $\pm$ 1.25	2.00	2.81 $\pm$ 0.64	4.00 $\pm$ 1.03	1.19
	30	12.14 $\pm$ 1.04	17.43 $\pm$ 1.21	5.29	5.52 $\pm$ 0.94	8.59 $\pm$ 0.31	3.07
7	1	12.78 $\pm$ 4.52	18.54 $\pm$ 3.83	5.76	0.78 $\pm$ 0.06	1.14 $\pm$ 0.18	0.36
	15	16.77 $\pm$ 1.97	24.04 $\pm$ 3.96	7.27	2.88 $\pm$ 0.20	4.97 $\pm$ 0.36	2.09
	30	16.66 $\pm$ 1.40	27.67 $\pm$ 3.11	11.01	5.55 $\pm$ 1.14	9.69 $\pm$ 2.06	4.14

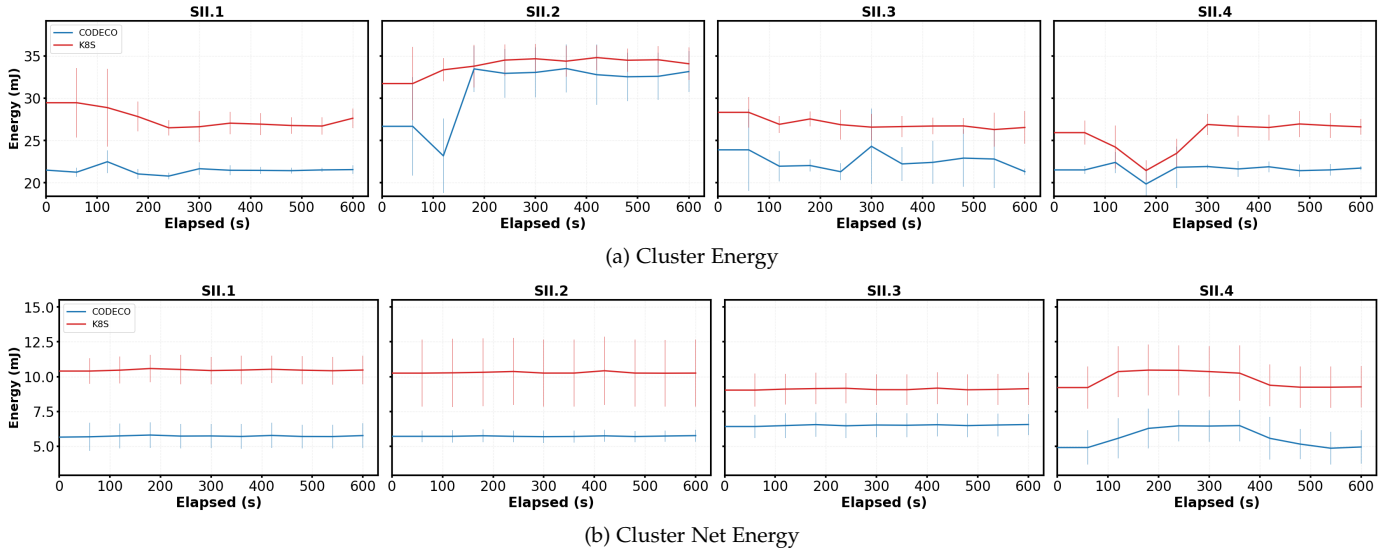


Fig. 8: Time-series evolution of cluster compute energy (top) and network energy (bottom) across sub-scenarios SII.1–SII.4 (rep = 7, RPS = 30).

However, unlike the baseline case in SII.1, the network-energy gap does not widen; instead, it narrows from approximately 4.5 mJ to approximately 2.5 mJ. This indicates that latency injection does not amplify K8s network-energy overhead in this experiment. Rather, CODECO remains more energy-efficient, although its relative network-energy advantage is reduced under the delay-injection condition.

**SII.4 Controlled Bandwidth Contention Impact.** Background `iperf3` traffic introduces visible transient behavior in both metrics. Compute energy dips briefly in both frameworks near 150s before recovering. After recovery, CODECO stabilises at approximately 22 mJ, while K8s stabilises at approximately 27 mJ. Network transmission energy rises transiently for CODECO to approximately 7.5 mJ during the congestion window before recovering toward its baseline level. In contrast, K8s remains elevated at approximately 10 mJ without a comparable recovery.

**SII Cross-scenario summary.** Across all four sub-scenarios, CODECO consistently results in lower compute cluster energy and network energy than K8s. Three patterns are observable in Figure 8. First, an improvement in regards to energy consumption due to computational resources is most stable and pronounced for the baseline case in SII.1 and for the network-delay case in SII.3, reflecting the effect of undisturbed placement decisions. Second, CPU stress in SII.2 temporarily narrows this advantage as CODECO migrates workloads. After migration, comp energy con-

sumption moves closer to the K8s level while still remaining lower.

As for the improvement concerning energy consumption due to packet transmission, it is stable throughout the migration event, indicating that co-location survives the fault-handling process. SII.4 is the only sub-scenario where CODECO’s network transmission energy rises transiently above its baseline, yet it recovers while K8s remains elevated. This suggests that the CODECO energy-aware placement strategy is more resilient to congestion than K8s.

### 6.3 Scenario III: Greenness Scheduling Strategies Comparison

Figure 9 presents the time-series evolution of cluster energy, network energy, and composite greenness scores for the three  $g(i)$  scheduling cost functions, under combined CPU and bandwidth stress.

**Computational energy.** All three  $g(i)$  functions produce broadly comparable cluster energy consumption throughout the experiments, with most values remaining around approximately 31 mJ. `comp` provides the lowest and most stable profile, staying close to approximately 30 mJ, which is consistent with its direct optimisation of computational cost. `net` exhibits a transient dip near 100s before recovering to approximately 33 mJ, while `green` fluctuates more visibly, reaching its lowest point at approximately 30 mJ and increasing to approximately 33 mJ near 350s. The narrow

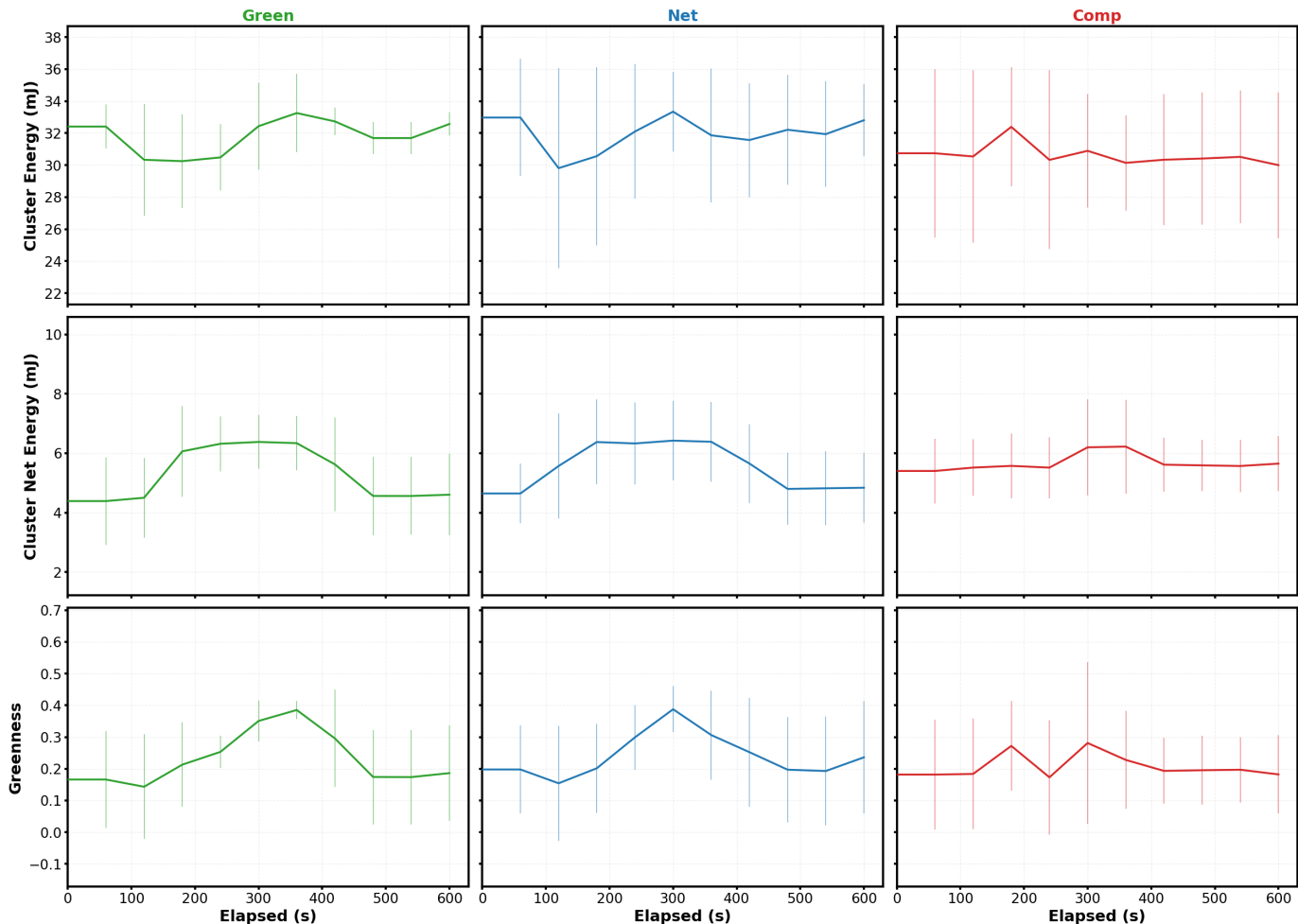


Fig. 9: Time-series evolution of cluster compute energy (top row), network energy (middle row), and greenness (bottom row) under combined CPU and bandwidth stress (S5) for the three CODECO scheduling objectives: *green*, *net* and *comp*.

spread across functions indicates that cluster-level computational energy is not strongly discriminated by the choice of  $g(i)$  under combined stress.

**Network energy.** Clearer differentiation emerges in network transmission energy consumption. *green* exhibits the most pronounced rise during the stress window, peaking at approximately 8 mJ before declining to approximately 6.5 mJ after 500 s. *net*, which explicitly targets transmission energy, rises transiently to approximately 7.3 mJ around 300 s but recovers more sharply, converging to approximately 5.8 mJ, the lowest post-stress value among the three functions. *comp* shows the flattest trajectory throughout the experiment, remaining close to approximately 6.5 mJ. Although it does not explicitly target network transmission, consolidating replicas for computational efficiency incidentally reduces inter-node flows, thereby stabilising transmission energy under combined fault conditions.

**Composite greenness as a ranking indicator.** The composite greenness score, defined as in Equation 5, consolidates both energy dimensions into a single indicator and is evaluated here as a tool for ranking the three  $g(i)$  functions. The score produces a consistent and stable ordering throughout the full 600 s window. *comp* achieves the lowest score, staying around approximately 0.15. *net* occupies the intermediate position, peaking at approximately 0.32 before

recovering to approximately 0.15. *green* scores highest, peaking at approximately 0.38 before declining to approximately 0.20.

The ordering reflects how each  $g(i)$  function affects the two constituent dimensions of the score. *comp* captures computational energy directly and, as a side effect, colocates replicas. This reduces inter-node flows and keeps network energy low, suppressing both dimensions of the score simultaneously and yielding the lowest composite value. *net* targets network transmission energy explicitly but does not constrain computational placement, leaving cluster energy higher and more variable. *green* jointly targets both dimensions. However, under simultaneous CPU and network stress, it receives conflicting cost signals from the two terms, preventing it from suppressing either dimension effectively. The network transmission term dominates the score at peak stress, producing the highest composite value despite the composite intent of the function.

The experiments run show that the composite greenness score is sensitive enough to discriminate the three scheduling functions and produce a stable cluster ranking under stress. However, the result also exposes a limitation of the composite  $g(i)$  formulation: jointly targeting both dimensions does not guarantee a joint energy advantage under concurrent fault conditions. Refinement, for instance

through adaptive weighting of the constituent terms based on the observed fault type, is needed before `green` can be reliably used as a scheduling objective in degraded edge environments.

#### 6.4 Analysis Summary and Discussion

The three scenarios collectively address three questions: i) whether CODECO reduces energy consumption relative to K8s; ii) which  $g(i)$  scheduling function performs best; and iii) whether the composite greenness score is an effective indicator for cluster ranking.

**Is CODECO more energy-efficient than K8s?** The results consistently support this claim. First, the advantage grows with replica count. This reflects CODECO’s application-first deployment model: the ILP solver places the full microservice graph jointly, prioritizing co-location over load balancing across nodes. Second, the two energy dimensions respond to different drivers. Network energy savings are governed primarily by RPS intensity as higher traffic amplifies the cost of inter-node flows generated by K8s’s distributed placement. Computational energy savings are governed primarily by replica count as more replicas mean more nodes partially loaded under K8s, while CODECO consolidates them onto fewer nodes. These two dimensions are therefore partially independent: a single-dimension  $g(i)$  function may leave savings in the other dimension unrealised, reinforcing the need to monitor both metrics separately when assessing overall energy efficiency.

Under fault conditions (Scenario II), the computational advantage narrows temporarily during workload migration but recovers, and the network energy gap is preserved across all sub-scenarios. This confirms that CODECO’s energy efficiency is robust to the injected fault conditions evaluated, including CPU stress, asymmetric network delay, and controlled bandwidth contention.

**Is there a best  $g(i)$  function?** No single  $g(i)$  formulation dominates unconditionally across all conditions, but a clear ordering emerges under combined stress. `comp` achieves the best outcome across all three cluster-level metrics: lowest computational energy, flattest network energy trajectory, and lowest composite greenness score. This is counterintuitive: a compute-only function outperforms the composite formulation on the composite metric. The reason is structural: co-locating replicas for computational efficiency simultaneously eliminates inter-node flows, suppressing network energy as a side effect. Both dimensions of the greenness score are therefore reduced without the  $g(i)$  function explicitly targeting either jointly.

`net` achieves the fastest post-stress recovery in network transmission energy ( $\approx 5.8$  mJ) and is preferable when rapid restoration of network efficiency after a fault is the operational priority. `green` performs worst during the fault period across all metrics: its composite cost function receives conflicting signals from both dimensions simultaneously under combined stress, preventing it from suppressing either effectively. In its current form it is least suited to degraded edge environments. It remains a candidate for stable, lightly loaded conditions where both cost signals are unambiguous and the joint optimisation does not face conflicting pressure.

The choice of  $g(i)$  should therefore be guided by the operational context: `comp` for sustained energy minimization under stress, `net` for fast post-fault network recovery, and `green` for undisturbed conditions or as a starting point for further refinement, for instance, through adaptive weighting of its constituent terms based on observed infrastructure state.

**Is the composite greenness score an effective ranking indicator?** The composite greenness score maintains a consistent ordering of the three  $g(i)$  functions across all experimentation, including during fault windows. This stability demonstrates that the score captures the joint energy behavior of each scheduling function and produces a reliable cluster ranking under stress. It is therefore more informative than either single-dimension metric alone when comparing scheduling strategies. However, when diagnosing the cause of a ranking outcome, the two constituent scores must be inspected separately: the composite value masks whether a high score is driven by computational overhead, network overhead, or both.

**Limitations.** Three additional aspects are worth noting. First, workload migration carries a non-negligible energy cost: the dip-and-recovery pattern observed under CPU stress temporarily converges CODECO’s cluster energy toward K8s levels. Frequent rescheduling in highly dynamic environments could erode the steady-state energy advantage, and migration-aware scheduling strategies that explicitly account for relocation overhead are an important direction for future work. Second, measurement fidelity on ARM-based embedded devices is limited: Kepler’s power model was trained on x86 hardware and provides only approximate estimates on Raspberry Pi 4 nodes, introducing a systematic uncertainty that affects all results equally but limits the precision of absolute energy values. Third, the Wi-Fi connectivity (IEEE 802.11bg) amplifies network energy differences relative to wired deployments; the advantage of co-location in eliminating inter-node transmission energy may be less pronounced in environments with lower per-packet transmission costs.

## 7 CONCLUSIONS AND NEXT STEPS

This work evaluates the energy efficiency of the K8s CODECO orchestration framework in a single-cluster far Edge deployment, focusing on how scheduling decisions affect both computational and network energy consumption. Three experimental scenarios are evaluated on a real-world ARM-based testbed, comparing CODECO against vanilla K8s across varying workload intensities, injected fault conditions, and alternative energy-aware scheduling functions.

The results consistently demonstrate that CODECO reduces cluster energy consumption relative to vanilla K8s. The advantage is driven by two independent mechanisms: CODECO’s ILP-based batch scheduler gives priority to an application dimension, thus co-locating communicating micro-service replicas, reducing the number of active nodes and eliminating inter-node Wi-Fi transmission for intra-application flows; and its reactive stateful migration mechanism reallocates workloads away from degraded nodes under fault conditions, preserving energy efficiency across CPU stress, asymmetric network delay, and bandwidth con-

tention. The benefit scales with replica count for computational energy, and with request rate for network energy, and is most pronounced at their combination.

Regarding the  $g(i)$  scheduling functions, no single formulation reaches a best target unconditionally. Under combined stress, the compute-only function (comp) achieves the best outcome across all three cluster-level metrics, including the composite greenness score, because co-locating for computational efficiency incidentally suppresses inter-node traffic as a side effect. The network function (net) recovers most rapidly in transmission energy after fault removal. The composite function (green) performs worst under combined stress, as simultaneous CPU and network degradation generates conflicting cost signals that prevent either dimension from being suppressed effectively. Finally, the composite greenness score proposed provides a stable and consistent ranking of the three functions throughout all experimental conditions, making it a reliable indicator for cluster-level energy assessment.

These findings point to three directions for future work.

**Migration-aware scheduling:** workload relocation carries a non-negligible energy cost that the current policy does not account for, and strategies that explicitly model and minimise the overhead of pod migration are needed for highly dynamic edge environments.

**Architecture-specific energy modeling:** Kepler’s power model was trained on x86 hardware and provides only approximate estimates on ARM-based embedded devices; retraining or calibrating the model against the target hardware would improve the fidelity of energy measurements and the accuracy of  $g(i)$  cost computations.

**Refinement of the  $g(i)$  scheduling heuristics:** the experiments confirm that the composite formulation is the most sensitive of the three scoring functions to concurrent fault conditions, as it responds to cost signals from both energy dimensions simultaneously. Under combined CPU and network stress this sensitivity produces higher variability in the greenness score, as neither dimension is fully suppressed when both are degraded at once. This same sensitivity, however, makes the composite  $g(i)$  the most promising candidate for refinement: a formulation that weights the constituent terms adaptively based on observed infrastructure state increasing the network weight under congestion, the computational weight under CPU stress, and rebalancing under combined conditions could make green the most responsive and accurate scheduling function across all operating conditions, rather than only under undisturbed operation. A further refinement direction is to incorporate migration cost explicitly into the  $g(i)$  formulation, so that the scheduler accounts for the energy overhead of workload relocation before triggering a migration, addressing the transient inefficiency observed under CPU stress in Scenario II. **Security-aware greenness scheduling:** The experiments presented in this paper are conducted on a controlled, isolated laboratory network and do not incorporate communication security overhead into the scheduling model. In real-world CEI deployments, encryption, mutual authentication, and secure overlay management — capabilities provided by the CODECO NetMA secure connectivity sub-component introduce non-trivial computational and transmission energy costs that vary with traffic volume

and cipher suite. Extending the  $g(i)$  scheduling heuristics to incorporate security-induced energy as an additional cost dimension is an open problem and a natural direction for future work, particularly in IIoT settings where both sustainability and confidentiality are operational requirements.

## ACKNOWLEDGEMENT

This work has been funded by The European Commission in the context of the Horizon Europe CODECO project under grant number 101092696, and by SGC, Grant agreement nr: M-0626, project SemComIIoT.

## REFERENCES

- [1] R. C. Sofia, J. Salomon, S. Ferlin-Reiter, L. Garcés-Erice, P. Urbanetz, H. Mueller, R. Touma, A. Espinosa, L. M. Contreras, V. Theodorou, N. Psaromanolakis, L. Mamatas, V. Tsaousidis, X. Fu, T. Yuan, A. del Rio, D. Jiménez, A. Stam, E. Paraskevoulakou, P. Karamolegkos, V. Vieira, J. Martrat, I. M. Prusiel, D. Matzakou, J. Soldatos, D. Remon, and M. Jahn, “A framework for cognitive, decentralized container orchestration,” *IEEE Access*, vol. 12, pp. 79978–80008, 2024.
- [2] R. C. Sofia, J. Salomon, R. Carrol, L. Garcés-Erice, P. Urbanetz, J. Gesswein, R. Touma, A. Espinosa, L. M. Contreras, V. Theodorou, G. Papanail, G. Koukis, V. Tsaousidis, A. del Rio, D. Jimenez, E. Paraskevoulakou, P. Karamolegkos, J. Soldatos, B. D. Nogales, and A. Tjaarda, “Towards scalable federated container orchestration: The codeco approach,” 2026.
- [3] J. Luo, L. Yin, J. Hu, C. Wang, X. Liu, X. Fan, and H. Luo, “Container-based fog computing architecture and energy-balancing scheduling algorithm for energy iot,” *Future Generation Computer Systems*, vol. 97, pp. 50–60, 2019.
- [4] Sustainable Computing, “Kepler: A sustainable computing framework,” 2023. Accessed: 2024-10-22.
- [5] D. Ali and R. C. Sofia, “Experimenting with energy-awareness in edge-cloud containerized application orchestration,” 2025.
- [6] Ł. Wojciechowski, K. Opasiak, J. Latusek, M. Wereski, V. Morales, T. Kim, and M. Hong, “Netmarks: Network metrics-aware kubernetes scheduler powered by service mesh,” in *IEEE INFOCOM 2021 - IEEE Conference on Computer Communications*, pp. 1–9, 2021.
- [7] X. Zhang, L. Li, Y. Wang, E. Chen, and L. Shou, “Zeus: Improving resource efficiency via workload colocation for massive kubernetes clusters,” *IEEE Access*, vol. 9, pp. 105192–105204, 2021.
- [8] Ragavan, Vivek Karunai Kiri and Nadig, Deepak, “Nas: A novel network-aware kubernetes scheduling framework using ebpf service mesh,” in *ICC 2025 - IEEE International Conference on Communications*, pp. 1512–1517, 2025.
- [9] Sofia, Rute C. (ed.), “D31: CODECO federated cluster operation architectural design,” May 2026.
- [10] Cloud Native Computing Foundation, “Exploring Kepler’s potentials: Unveiling cloud application power consumption,” Oct. 2023. Accessed: 2024-11-13.
- [11] L. Ardito and M. Torchiano, “Creating and evaluating a software power model for Linux single board computers,” in *Proceedings of the 6th International Workshop on Green and Sustainable Software, GREENS ’18*, (New York, NY, USA), pp. 1–8, Association for Computing Machinery, 2018.
- [12] T. Pol, “Carbon footprint monitoring up to container-level in virtualized environments: A hardware and hypervisor-free approach,” 2024. Accessed: 2024-04-12.
- [13] L. M. Feeney and M. Nilsson, “Investigating the energy consumption of a wireless network interface in an ad hoc networking environment,” in *Proceedings IEEE INFOCOM 2001. Conference on Computer Communications. Twentieth Annual Joint Conference of the IEEE Computer and Communications Society*, vol. 3, pp. 1548–1557, 2001.